Electrical Power and Energy Systems 136 (2022) 107685

Contents lists available at ScienceDirect

International Journal of Electrical Power and Energy Systems

journal homepage: www.elsevier.com/locate/ijepes

Offering and bidding for a wind producer paired with battery and CAES units considering battery degradation

Hooman Khaloie [a], Amjad Anvari-Moghaddam [b,*], Javier Contreras [c], Jean-François Toubeau [a], Pierluigi Siano [d,e], François Vallée [a]

[a] Power Systems & Markets Research Group, University of Mons, Mons, Belgium
[b] Department of Energy (AAU Energy), Aalborg University, 9220 Aalborg East, Denmark
[c] Escuela Técnica Superior de Ingenieros Industriales, University of Castilla–La Mancha, Ciudad Real 13071, Spain
[d] Department of Management & Innovation Systems, University of Salerno, Fisciano, Italy
[e] Department of Electrical and Electronic Engineering Science, University of Johannesburg, Johannesburg, South Africa

ARTICLE INFO

Keywords:
Battery energy storage (BES)
Compressed air energy storage (CAES)
Electricity market
Offering and bidding strategies
Wind farm

ABSTRACT

This paper presents a stochastic framework for offering and bidding strategies of a hybrid power generation system (HPGS) with a wind farm and two types of energy storage facilities, i.e., compressed air energy storage (CAES) and battery energy storage (BES) systems. The model considers the participation of the HPGS in consecutive electricity markets, i.e., day-ahead (DA) and intraday markets. To better address the proposed trading strategy problem, the BES degradation cost is also incorporated into the model. Furthermore, a mechanism based on energy procurement from demand response resources (DRRs) in the intraday demand response exchange (IDREX) market for the HPGS is also established to offset unexpected energy imbalances effectively. The suggested offering and bidding strategy is formulated as a three-stage stochastic programming problem incorporating a risk-alleviating index, namely, the conditional value-at-risk (CVaR). Results from several simulations indicate considerable profit gain and risk reduction achieved by the suggested offering and bidding framework.

1. Introduction

Lessening dependence on fossil fuels and taking maximum advantage of renewable energy sources to reduce greenhouse gas emissions has become one of the main goals of communities and governments around the world [1]. Moving toward a fully renewable energy power sector without appropriate energy storage systems and flexible loads is unattainable [2]. The importance of energy storage systems in reaching a fully renewable energy power sector in the next 30 years for Europe has been investigated in [3]. The results of [3] reveal that energy storage technologies are able to play a crucial part in reducing the levelized cost of electricity.

With the enormous growth of renewable energy sources, such as wind energy, in all power system sectors, designing appropriate offering strategies for optimal participation in the electricity markets is identified as the most prominent concern of their owners [4]. In particular, the intermittent nature of prominent renewable energy resources such as wind turbines is the origin of all these challenges and concerns. In [5], the authors have focused on the operating framework of a wind power plant in the day-ahead (DA) energy and reserve markets based on deep reinforcement learning. The application of second-order stochastic dominance constraints as the risk handling method for the optimal participation of a wind power plant has been proposed in [6]. The optimal participation model for paired wind power plants and demand response providers has been presented in [7]. Similarly, optimal behavior of a renewable-based power plant having a demand response provider was studied in [8]. In [9], the authors have suggested an offering framework for wind and thermal units participating in day-ahead, medium-term, and long-term electricity markets.

Other electricity market players, such as microgrids and virtual power plants, are also found in the bidding and offering strategy problems. Authors in [10] have designed a two-stage bidding structure for a microgrid based on the mean–variance model. Following this, a bidding strategy based on information gap decision theory (IGDT) and stochastic programming for a reconfigurable microgrid in the DA and real-time markets has been suggested in [11]. Analogous to [11], in [12] and [13], the IGDT method was applied for the self-scheduling of a virtual power plant in joint DA and balancing markets, respectively. In [13], the authors have presented a risk-based scheduling model for

* Corresponding author.
E-mail address: aam@energy.aau.dk (A. Anvari-Moghaddam).

https://doi.org/10.1016/j.ijepes.2021.107685
Received 6 October 2020; Received in revised form 8 August 2021; Accepted 1 October 2021
Available online 1 November 2021

Nomenclature

Indices

θ	Index of scenarios (1 to N_θ).
t	Index of scheduling periods (1 to N_T).
d	Index of DRRs (1 to N_D).
f	Index pertaining to segments of DRRs' offer (1 to N_F).
b	Index pertaining to blocks of the BES depth of discharge (1 to N_B).

Parameters

π_θ	Probability of a scenario occurrence.
β (α)	Parameters reflecting the risk-aversion (confidence) level.
$\varphi^{B}_{d,t}$	Price of the bilateral contract between DRRs and the HPGS, €/MWh.
$\varphi^{IX}_{d,f,t}$	Price pertaining to segments of the DRRs' offer in the IDREX market, €/MWh.
$Cap^{BS,dis(ch)}$	Maximum discharging (charging) quantity of the BES, MW.
$Cap^{CA,c}$	Maximum compression quantity of the CAES, MW.
$Cap^{CA,exp}$	Maximum expansion quantity of the CAES, MW.
Cap^{W}	Nominal capacity of the wind farm, MW.
$EL^{BS(CA),Max}$	Maximum permissible stored energy in the BES (CAES), MWh.
$ELL^{BS,Max}$	Maximum permissible stored energy in block b of the depth of BES discharge of the system, MWh.
$\Upsilon^{BS,ch(dis)}$	BES efficiency pertaining to charging (discharging) mode.
$Htr^{dis(s)}$	CAES heat rate in discharging (simple-cycle) mode, MBtu/MWh.
NPG	Price of natural gas, €/MBtu.
$OM^{Exp(Com)}$	Maintenance and operation costs of the CAES in expanding (compressing) mode, €/MWh.
ER	CAES energy ratio.
λ	A coefficient for determining the contribution level in the intraday market.
$v^{Max}_{d,f,t}$	Maximum purchased power in each segment of the DRR's offering curve, MW.
Cap^{DR}_{d}	Total offering quantity by each DRR, MW.
$Cap^{I,HPGS,sell}$	Maximum allowable selling power by the HPGS system in the intraday market, MW.
$Cap^{I,HPGS,buy}$	Maximum allowable buying power by the HPGS system in the intraday market, MW.
MC_b	Marginal cost of degradation in block b of the depth of discharge of the BES system.

Variables

γ	Value-at-risk, €.
$\varphi^{D(I)}_{t,\theta}$	Price pertaining to the DA (intraday) market, €/MWh.
$\chi^{D(I),W}_{t,\theta}$	Offering quantity from the wind farm in the DA (intraday) market, MW.
$\chi^{D(I),BS}_{t,\theta}$	Offering quantity from the BES system in the DA (intraday) market, MW.
$\chi^{D,CA,dis(s)}_{t,\theta}$	DA offering quantity from the CAES system in the discharging (simple-cycle) mode, MW.
$\chi^{I,CA,dis(s)}_{t,\theta}$	Intraday offering quantity from the CAES system in the discharging (simple-cycle) mode, MW.
$\sigma^{D,BS(CA)}_{t,\theta}$	Bidding quantity from the BES (CAES) system in the DA market, MW.
$\sigma^{I,BS(CA)}_{t,\theta}$	Bidding quantity from the BES (CAES) system in the intraday market, MW.
$\sigma^{I,W}_{t,\theta}$	Buying quantity from the wind farm in the intraday market, MW.
$\chi^{Sch,BS(CA),dis}_{t,\theta}$	Final scheduled power of the BES (CAES) system in the discharging mode, MW.
$\chi^{Sch,CA,s}_{t,\theta}$	Final scheduled power of the CAES system in the simple-cycle mode, MW.
$\sigma^{Sch,BS(CA),ch}_{t,\theta}$	Final scheduled power of the BES (CAES) system in the charging mode, MW.
$P^{Sch,HPGS}_{t,\theta}$	Final scheduled power of the HPGS, MW.
$\varrho^{D(I),BS,dis}_{b,t,\theta}$	Offering quantity of the BES system from block b of the depth of discharge in DA (intraday) market, MW.
$\varrho^{D(I),BS,ch}_{b,t,\theta}$	Bidding quantity of the BES system from block b of the depth of discharge in DA (intraday) market, MW.
$\varrho^{Sch,BS,dis(ch)}_{b,t,\theta}$	Final scheduled power of the BES system from block b of the depth of discharge in discharging (charging) mode, MW.
$ELL^{BS}_{b,t,\theta}$	Stored energy in block b of the depth of discharge of the BES system, MWh.
$EL^{BS(CA)}_{t,\theta}$	Stored energy in the BES (CAES) system, MWh.
$RP^{W}_{t,\theta}$	Realized generation power of the wind farm, MW.
$\delta^{-(+)}_{t,\theta}$	Downward (upward) imbalance, MWh.
$\delta_{t,\theta}$	Final energy deviations of the HPGS, MWh.
$\rho^{-(+)}_{t,\theta}$	Price ratios pertaining to downward (upward) imbalances.
η_θ	Subsidiary variable used for CVaR calculation.
$v^{ch(dis)}_{t}$	Binary variable reflecting the charging (discharging) status of the BES.
$u^{ch/dis/s}_{t}$	Binary variable reflecting the charging/discharging/simple-cycle status of the CAES.
$CDR_{d,t,\theta}$	Cost pertaining to buying pool-based demand response (DR) from DRRs, €.
$DR_{d,t,\theta}/\chi^{B,DR}_{d,t,\theta}$	Provided pool-based/bilateral-based DR from DRRs, MW.
$CF^{CA}_{d,t,\theta}$	Cost pertaining to the CAES operation, €.

a virtual power plant participating in day-ahead energy and reserve markets. Authors in [14] have focused on the stochastic self-scheduling of a smart microgrid in the DA market.

Energy storage technologies are other inevitable facilities in all power systems that bring more flexibility and reduce overall costs. A comprehensive stochastic-robust participation framework for a battery energy storage (BES) system has been introduced in [15]. Furthermore, an offering model for joint operation of the BES system and a solar plant employing adjustable robust optimization technique has been analyzed in [16]. A further mechanism for the trading strategy of a BES system along with thermal units and a wind power station considering environmental issues has been provided in [17]. Ref. [18] has provided

a linear deterministic look-ahead optimization model for the optimal involvement of a compressed air energy storage (CAES) system in multiple electricity markets. A coordinated operation mechanism based on the adaptive robust technique for a wind-CAES system has been developed in [19]. Moreover, a stochastic offering mechanism for a wind-CAES plant has been presented in [20]. In [21], the authors have focused on expanding a coordinated trading method for a wind power station and electric vehicles in DA and intraday markets.

The risk-based behavior of thermal units using under the uncertainty of high-impact low-probability events under a hybrid probabilistic–possibilistic approach [22] has been presented in [23]. The impact of transmission outage contingencies on the bidding strategy of thermal units has been assessed in [24]. In [25], authors have provided an scheduling model for a hybrid thermal-BES system while dealing with the existing uncertainty using robust optimization. A stochastic bidding structure for a price-maker retailer in the DA trading floor has been provided in [26]. Authors in [27] have developed a bi-level self-scheduling paradigm for power-to-gas facilities in the DA market. In [28] and [29], authors have assessed the demand response resources (DRRs) bidding strategy from various perspectives. In [28], a robust framework has been applied for the bidding strategy of industrial DRRs, whereas [29] has concentrated on the trading approach of residential DRRs.

In this paper, a comprehensive offering and bidding model for a hybrid power generation system (HPGS) composed of wind farms, CAES, and BES system is presented. In addition to the benefits of coordination among offering and bidding of all resources, a mechanism based on the energy transaction between the HPGS and DRRs is considered. The suggested model takes into account the DA market, the intraday market, and the balancing market as intended trading floors. In this regard, the proposed structure is not only capable of extracting selling offers (offering curves), but also provides the ability to derive the purchasing bids (bidding curves) in the DA market. The present offering and bidding mechanism is developed as a three-stage stochastic programming pattern while the uncertainties arising from the electricity prices and wind generation are characterized through a scenario set. Lastly, to further investigate the different offering and bidding schemes in the decision-making process, an effective risk metric, i.e., conditional value-at-risk (CVaR) is included in the framework.

The main innovative contributions of this work are as follows:

- Proposing a comprehensive model for the joint operation of a wind farm, BES, and a CAES system in the form of an HPGS for participation in successive electricity markets. To the best of the authors' knowledge, there is no relevant publication that addresses the integrated operation of wind, CAES, and BES system in electricity markets. It is important to note that the wind-CAES offering model proposed in [20] suffers from two weaknesses in its methodology: (1) the authors considered the charging power of the CAES in the scheduled power of the integrated wind-CAES system, while it should not be regarded (in other words, the charging energy is utilized for increasing the energy level of the storage systems, and it must not be calculated in the scheduled energy of the HPGS for coping with its balancing market deviations) and (2) the operating modes of the CAES facility must be counted in modeling the upper bound of the system's downward imbalance, while they have been neglected in [20].
- Presenting a novel three-stage stochastic trading model which is capable of deriving both offering (selling) and bidding (purchasing) curves in the DA market. Other significant difference between this paper and the methodology proposed in [20] is that the operating modes of the CAES facility, i.e., charging, discharging, simple-cycle, have been considered as a function of stochastic scenarios, while this assumption cannot represent the real operation of a CAES unit.
- Providing energy transaction capability between the HPGS and DRRs by means of the intraday demand response exchange (IDREX) market and thoroughly examining this facility on the operation of all resources, especially BES and CAES systems.
- Incorporating the BES degradation cost into the suggested offering and bidding architecture and analyzing its influence from the perspective of coordinated and uncoordinated operations.
- Analyzing different aspects of the proposed risk-based offering and bidding strategy with a detailed numerical result.

In the next section, materials and methods are discussed. Section 3 presents the simulation results and discussion, and the last section is dedicated to the conclusion and future work.

2. Materials and methods

2.1. Decision-making framework

As stated in the previous section, the HPGS aims for an optimal participation in the DA and intraday markets, as two consecutive trading floors. In order to achieve optimal operation of the HPGS in all trading floors, system uncertainties must be well addressed. Generally, the system uncertainties concern the DA market, intraday market, and balancing market prices along with wind power generation. Multi-stage stochastic programming is one of the most prevailing methodologies for addressing uncertainties, and this has been properly adapted to electricity market problems [30]. In this work, a three-stage stochastic programming structure is employed whose corresponding decision variables are categorized into three stages:

1. **First stage:** the first-stage decisions concern the operating status of the BES and CAES systems, and optimal offering and bidding curves of the HPGS in the DA market for the whole scheduling horizon. These decisions are called *here-and-now* decisions that are made while all uncertain parameters are unknown to the HPGS.
2. **Second stage:** these decisions deal with buying and selling energy in the intraday market along with traded pool-based and bilateral-based demand response (DR) between DRRs and the HPGS. These decisions depend on the DA market scenarios while the intraday market prices, balancing prices, and wind power production are still unknown at this stage. The set of the second-stage decisions are called *wait-and-see*1.
3. **Third stage:** the last stage decisions are related to balancing market deviations of the HPGS. These decisions are named *wait-and-see*2 and are made after satisfying all uncertain variables.

For the stochastic modeling of the uncertain sources, proper probability distribution functions are chosen. Normal and Rayleigh probability distributions are picked to model market prices and wind speed, respectively. Next, the roulette wheel technique is implemented for scenario generation [31]. Since running multi-stage stochastic programming problems with a large amount of scenarios results in a significant computational burden, a scenario reduction technique, by means of Kantorovich distance, is utilized [32].

In the next part, first, the mathematical formulation of the HPGS trading behavior in DA and intraday trading floors is thoroughly given. Then, the aforementioned formulation is updated considering the BES degradation cost.

2.2. Problem formulation in the absence of degradation cost

The aim of the offering and bidding mechanism for the HPGS is to maximize the expected profit throughout the scheduling horizon. This includes a coordinated decision-making system for all available resources, i.e., wind farm, BES, and CAES, that specifies the optimal participation of all units in the DA and intraday trading floors. In order

to handle the risk associated with stochastic parameters, the CVaR metric is considered in the proposed structure. A graphical overview of the developed methodology is shown in Fig. 1. The objective function of the HPGS offering and bidding strategy can be written as (1).

$$\begin{aligned}\text{Max}\quad \text{PF}_1 = \sum_{\Theta=1}^{N_\theta}\sum_{t=1}^{N_T}\pi_\theta \times \Big[& \varphi^D_{t,\theta}\chi^{D,W}_{t,\theta} + \varphi^D_{t,\theta}\chi^{D,BS}_{t,\theta} + \varphi^D_{t,\theta}\chi^{D,CA,dis}_{t,\theta} \\ & + \varphi^D_{t,\theta}\chi^{D,CA,s}_{t,\theta} \\ & - \varphi^D_{t,\theta}\sigma^{D,BS}_{t,\theta} - \varphi^D_{t,\theta}\sigma^{D,CA}_{t,\theta} + \varphi^I_{t,\theta}\chi^{I,W}_{t,\theta} \\ & + \varphi^I_{t,\theta}\chi^{I,BS}_{t,\theta} + \varphi^I_{t,\theta}\chi^{I,CA,dis}_{t,\theta} + \varphi^I_{t,\theta}\chi^{I,CA,s}_{t,\theta} \\ & - \varphi^I_{t,\theta}\sigma^{I,W} - \varphi^I_{t,\theta}\sigma^{I,BS}_{t,\theta} - \varphi^I_{t,\theta}\sigma^{I,CA}_{t,\theta} \\ & - \left(\sum_{d=1}^{N_D} CDR_{d,t,\theta} + \varphi^B_{d,t}\chi^{B,DR}_{d,t,\theta}\right) \\ & - CF^{CA}_{t,\theta} + \left(\varphi^D_{t,\theta}\rho^+_{t,\theta}\delta^+_{t,\theta}\right) - \left(\varphi^D_{t,\theta}\rho^-_{t,\theta}\delta^-_{t,\theta}\right)\Big] \\ & + \beta\left(\gamma - \frac{1}{1-\alpha}\sum_{\Theta=1}^{N_\theta}\pi_\theta\eta_\theta\right)\end{aligned} \tag{1}$$

where PF_1 refers to the objective function of the HPGS without considering the BES degradation cost. The objective function (1) is written in three rows, and each row comprises various terms. The first row represents the revenue of the HPGS due to the participation of wind, battery, and CAES units in the DA market. The first two terms of the second row are related to purchasing bids of BES and CAES systems from the DA market. The next four terms in the same row correspond to the HPGS revenue from the intraday market arising from selling energy. The third row refers to the costs for acquiring energy from the intraday market and procurement of pool-based and bilateral-based DR from the IDREX market. The first term in the last row models the CAES operational costs, while the next two expressions denote the income and costs related to balancing market deviations. Finally, the last term of the fourth row represents the risk term in which higher values of β reflect the increasing importance of the risk aversion. The constraints of objective function (1) are described as follows:

2.2.1. CVaR constraints

Restrictions (2)–(4) are utilized to calculate the CVaR.

$$\begin{aligned}\text{PF}_{1,\theta} = \sum_{t=1}^{N_T}\Big[& \varphi^D_{t,\theta}\chi^{D,W}_{t,\theta} + \varphi^D_{t,\theta}\chi^{D,BS}_{t,\theta} + \varphi^D_{t,\theta}\chi^{D,CA,dis}_{t,\theta} \\ & + \varphi^D_{t,\theta}\chi^{D,CA,s}_{t,\theta} - \varphi^D_{t,\theta}\sigma^{D,BS}_{t,\theta} - \varphi^D_{t,\theta}\sigma^{D,CA}_{t,\theta} + \varphi^I_{t,\theta}\chi^{I,W}_{t,\theta} \\ & + \varphi^I_{t,\theta}\chi^{I,BS}_{t,\theta} + \varphi^I_{t,\theta}\chi^{I,CA,dis}_{t,\theta} + \varphi^I_{t,\theta}\chi^{I,CA,s}_{t,\theta} - \varphi^I_{t,\theta}\sigma^{I,W} \\ & - \varphi^I_{t,\theta}\sigma^{I,BS}_{t,\theta} - \varphi^I_{t,\theta}\sigma^{I,CA}_{t,\theta} - \left(\sum_{d=1}^{N_D} CDR_{d,t,\theta} + \varphi^B_{d,t}\chi^{B,DR}_{d,t,\theta}\right) \\ & - CF^{CA}_{t,\theta} + \left(\varphi^D_{t,\theta}\rho^+_{t,\theta}\delta^+_{t,\theta}\right) - \left(\varphi^D_{t,\theta}\rho^-_{t,\theta}\delta^-_{t,\theta}\right)\Big]\end{aligned} \tag{2}$$

$$-\text{PF}_{1,\theta} + \gamma - \eta_\theta \le 0, \quad \forall\theta \tag{3}$$

$$\eta_\theta \ge 0, \quad \forall\theta \tag{4}$$

In (2), $\text{PF}_{1,\theta}$ calculates the profit per scenario of the HPGS in each scheduling period. Constraint (3) enforces that the difference between value-at-risk (γ) and profit per scenario ($\text{PF}_{1,\theta}$) should be lower than a positive subsidiary variable (η_θ). This positive subsidiary variable (η_θ) assists decision-makers in calculating the CVaR under a predefined confidence level (α) [32,33].

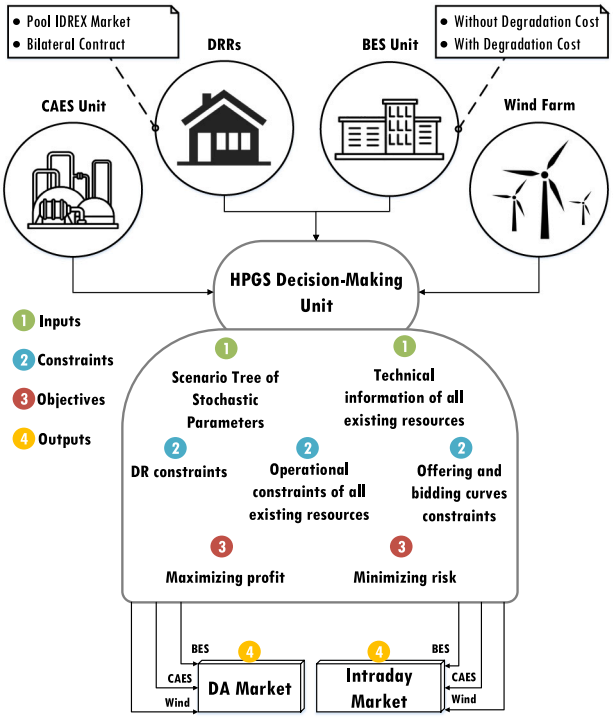

Fig. 1. Graphical overview of the proposed architecture.

2.2.2. BES operating constraints

Constraints (5) and (6) calculate the whole scheduled discharging and charging powers. Restrictions (7) and (8) enforce upper and lower limits on the whole BES scheduled power in any of the running modes, whereas constraint (9) ensures that the BES operates either in discharging or charging situations in any particular time interval. The energy level of the BES at time interval t is computed in (10), and subsequently, constraint (11) expresses the stored energy limits of the BES [34].

$$\chi^{Sch,BS,dis}_{t,\theta} = \chi^{D,BS}_{t,\theta} + \chi^{I,BS}_{t,\theta}, \quad \forall t, \forall\theta \tag{5}$$

$$\sigma^{Sch,BS,ch}_{t,\theta} = \sigma^{D,BS}_{t,\theta} + \sigma^{I,BS}_{t,\theta}, \quad \forall t, \forall\theta \tag{6}$$

$$0 \le \chi^{Sch,BS,dis}_{t,\theta} \le Cap^{BS,dis}\upsilon^{dis}_t, \quad \forall t, \forall\theta \tag{7}$$

$$0 \le \sigma^{Sch,BS,ch}_{t,\theta} \le Cap^{BS,ch}\upsilon^{ch}_t, \quad \forall t, \forall\theta \tag{8}$$

$$\upsilon^{dis}_t + \upsilon^{ch}_t \le 1, \quad \forall t \tag{9}$$

$$\begin{aligned}EL^{BS}_{t,\theta} = & EL^{BS}_{t-1,\theta} - \left(\frac{1}{\Upsilon^{BS,dis}}\right)\left(\chi^{Sch,BS,dis}_{t,\theta}\right) + \\ & \Upsilon^{BS,ch}\left(\sigma^{Sch,BS,ch}_{t,\theta}\right), \quad \forall t, \forall\theta\end{aligned} \tag{10}$$

$$0 \le EL^{BS}_{t,\theta} \le EL^{BS,Max}, \quad \forall t, \forall\theta \tag{11}$$

2.2.3. CAES operating constraints

One of the significant advantages of the CAES versus BES is the ability to generate energy in simple-cycle mode, similar to a gas turbine, which increases its flexibility against price fluctuation. Eqs. (12)–(14) are respectively concerned with the whole scheduled power of the CAES in discharging, simple-cycle, and charging modes. CAES operating costs are modeled using (15). Constraint (16) imposes that the CAES system should not be simultaneously in charging, discharging, and simple-cycle modes at any specific time interval. Restrictions pertaining

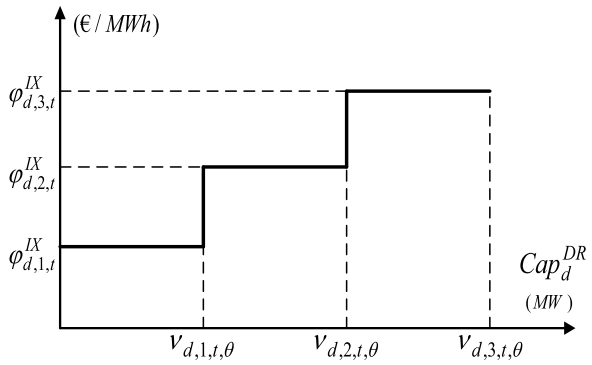

Fig. 2. Price–quantity offer of a DRR in the IDREX market.

to total scheduled power of the CAES system are enforced through (17)–(19). Finally, Eq. (20) calculates the energy level of the CAES, while constraint (21) keeps the energy level within the allowable range.

$$\chi^{Sch,CA,dis}_{t,\theta} = \chi^{D,CA,dis}_{t,\theta} + \chi^{I,CA,dis}_{t,\theta}, \quad \forall t, \forall \theta \tag{12}$$

$$\chi^{Sch,CA,s}_{t,\theta} = \chi^{D,CA,s}_{t,\theta} + \chi^{I,CA,s}_{t,\theta}, \quad \forall t, \forall \theta \tag{13}$$

$$\sigma^{Sch,CA,ch}_{t,\theta} = \sigma^{D,CA}_{t,\theta} + \sigma^{I,CA}_{t,\theta}, \quad \forall t, \forall \theta \tag{14}$$

$$\begin{aligned} CF^{CA}_{t,\theta} =& \chi^{Sch,CA,dis}_{t,\theta}\left(Htr^{dis}NPG + OM^{Exp}\right) \\ &+ \chi^{Sch,CA,s}_{t,\theta}\left(Htr^{s}NPG + OM^{Exp} + OM^{Com}\right) \\ &+ \sigma^{Sch,CA,ch}_{t,\theta}\left(OM^{Com}\right), \quad \forall t, \forall \theta \end{aligned} \tag{15}$$

$$u^{dis}_{t} + u^{s}_{t} + u^{ch}_{t} \le 1, \quad \forall t \tag{16}$$

$$0 \le \chi^{Sch,CA,dis}_{t,\theta} \le Cap^{CA,exp}u^{dis}_{t}, \quad \forall t, \forall \theta \tag{17}$$

$$0 \le \chi^{Sch,CA,s}_{t,\theta} \le Cap^{CA,exp}u^{s}_{t}, \quad \forall t, \forall \theta \tag{18}$$

$$0 \le \sigma^{Sch,CA}_{t,\theta} \le Cap^{CA,c}u^{ch}_{t}, \quad \forall t, \forall \theta \tag{19}$$

$$EL^{CA}_{t,\theta} = EL^{CA}_{t-1,\theta} + ER\left(\chi^{Sch,CA,dis}_{t,\theta} - \sigma^{Sch,CA}_{t,\theta}\right), \forall t, \forall \theta \tag{20}$$

$$0 \le EL^{CA}_{t,\theta} \le EL^{CA,Max}, \quad \forall t, \forall \theta \tag{21}$$

2.2.4. DR constraints

The proposed DR model includes energy procurement by the HPGS from DRRs in the IDREX market. In this regard, the HPGS can procure the intended energy either in the pool IDREX market or directly through bilateral contracts with DRRs. DRRs submit their price–quantity offers (Fig. 2) in the IDREX market, which corresponds to load reduction at each level ($v_{d,f,t,\theta}$) and the corresponding price ($\varphi^{IX}_{d,f,t}$). Eqs. (22) and (23) calculate the total procured energy from each DRR and its corresponding cost, respectively. Constraint (24) restricts the procured pool-based DR within its attainable capacity in every quantity segment. Ultimately, the total procured DR by the HPGS, i.e., the sum of pool-based and bilateral-based DR, is limited by applying restriction (25).

$$DR_{d,t,\theta} = \sum_{f=1}^{N_F} v_{d,f,t,\theta}, \quad \forall d, \forall t, \forall \theta \tag{22}$$

$$CDR_{d,t,\theta} = \sum_{f=1}^{N_F} (\varphi^{IX}_{d,f,t})(v_{d,f,t,\theta}), \quad \forall d, \forall t, \forall \theta \tag{23}$$

$$v_{d,f,t,\theta} \le v^{Max}_{d,f,t}, \quad \forall d, \forall f, \forall t, \forall \theta \tag{24}$$

$$DR_{d,t,\theta} + \chi^{B,DR}_{d,t,\theta} \le Cap^{DR}_{d}, \quad \forall d, \forall t, \forall \theta \tag{25}$$

2.2.5. Imbalance constraints

Total balancing market deviations of the HPGS are calculated using Eqs. (26) and (27). Positive and negative energy deviations of the HPGS are limited via constraints (28) and (29), respectively. It is worth to note that the operating modes of storage facilities must be counted in constraint (29), as the maximum negative energy deviation of the HPGS is equivalent to the maximum capacity of generating energy in each specific hour, while this rule has been ignored in [20].

$$\delta_{t,\theta} = \delta^{+}_{t,\theta} - \delta^{-}_{t,\theta}, \quad \forall t, \forall \theta \tag{26}$$

$$\begin{aligned} \delta_{t,\theta} =& RP^{W}_{t,\theta} + \chi^{Sch,BS,dis}_{t,\theta} + \chi^{Sch,CA,dis}_{t,\theta} + \chi^{Sch,CA,s}_{t,\theta} \\ &- P^{Sch,HPGS}_{t,\theta}, \quad \forall t, \forall \theta \end{aligned} \tag{27}$$

$$\begin{aligned} &\delta^{+}_{t,\theta} \le RP^{W}_{t,\theta} + \chi^{Sch,BS,dis}_{t,\theta} + \chi^{Sch,CA,dis}_{t,\theta} + \chi^{Sch,CA,s}_{t,\theta}, \\ &\forall t, \forall \theta \end{aligned} \tag{28}$$

$$\begin{aligned} \delta^{-}_{t,\theta} \le& Cap^{W} + \left(Cap^{BS,dis}v^{dis}_{t}\right) + \left(Cap^{CA,exp}u^{dis}_{t}\right) \\ &+ \left(Cap^{CA,exp}u^{s}_{t}\right), \quad \forall t, \forall \theta \end{aligned} \tag{29}$$

2.2.6. Offering and bidding curve constraints

DA offering and bidding limitations are imposed through constraints (30) and (31), respectively. Constraints (32) and (33) enforce the selling and buying quantities of the HPGS in the intraday market. It is important to bear in mind that market players cannot sell/procure their full capacity in/from the intraday market [32], and accordingly, these selling and buying restrictions are defined in Eqs. (34) and (35). The scheduled power of the HPGS in DA and intraday markets and its corresponding limits are specified in constraints (36) and (37), respectively. Unlike [20], in Eq. (36), the charging power of storage facilities should not be counted. In other words, the charging energy is utilized for increasing the energy level of the storage systems, and it must not be calculated in the scheduled energy of the HPGS for coping with its balancing market deviations. Deriving optimal offering and bidding curves in the DA market is the most substantial part of the problem. To this end, the offering curves must be non-decreasing while the bidding curves should be decreasing [8]. Constraints (38) and (39) ensure that the offering and bidding curves in the DA follow this trend. Lastly, the non-anticipativity condition of offering and bidding curves in the DA market, as well as non-anticipativity restrictions of offering and bidding quantities in the intraday trading floor, are enforced through constraints (40)–(43) [35].

$$\begin{aligned} &0 \le \chi^{D,\Gamma_1}_{t,\theta} \le Cap^{\Gamma_1}, \quad \forall t, \forall \theta \\ &\& \quad \Gamma_1 = \left[W, (BS,dis), (CA,dis), (CA,s)\right] \end{aligned} \tag{30}$$

$$0 \le \sigma^{D,\Gamma_2}_{t,\theta} \le Cap^{\Gamma_2}, \quad \forall t, \forall \theta \qquad \Gamma_2 = \left[(BS,ch), (CA,ch)\right] \tag{31}$$

$$\begin{aligned} &0 \le \chi^{I,W}_{t,\theta} + \chi^{I,BS,dis}_{t,\theta} + \chi^{I,CA,dis}_{t,\theta} + \chi^{I,CA,s}_{t,\theta} \le Cap^{I,HPGS,sell}, \\ &\forall t, \forall \theta \end{aligned} \tag{32}$$

$$\begin{aligned} &0 \le \sigma^{I,W}_{t,\theta} + \sigma^{I,BS,ch}_{t,\theta} + \sigma^{I,CA,ch}_{t,\theta} \le Cap^{I,HPGS,buy}, \\ &\forall t, \forall \theta \end{aligned} \tag{33}$$

$$Cap^{I,HPGS,sell} = \lambda\left(Cap^{W} + Cap^{BS,dis} + Cap^{CA,exp}\right) \tag{34}$$

$$Cap^{I,HPGS,buy} = \lambda\left(Cap^{W} + Cap^{BS,ch} + Cap^{CA,c}\right) \tag{35}$$

$$\begin{aligned} P^{Sch,HPGS}_{t,\theta} =& \chi^{D,W}_{t,\theta} + \chi^{I,W}_{t,\theta} - \sigma^{I,W}_{t,\theta} + \chi^{Sch,BS,dis}_{t,\theta} \\ &+ \chi^{Sch,CA,dis}_{t,\theta} + \chi^{Sch,CA,s}_{t,\theta} \end{aligned}$$

$$- \sum_{d=1}^{N_D} \left(DR_{d,t,\theta} + \chi_{d,t,\theta}^{B,DR} \right), \ \forall t, \forall \theta \tag{36}$$

$$P_{t,\theta}^{Sch,HPGS} \leq Cap^{W} + \left(Cap^{BS,dis} \upsilon_t^{dis} \right) + \left(Cap^{CA,exp} u_t^{dis} \right) + \left(Cap^{CA,exp} u_t^{s} \right), \quad \forall t, \forall \theta \tag{37}$$

$$\chi_{t,\theta}^{D,\Gamma_3} \leq \chi_{t,\widetilde{\theta}}^{D,\Gamma_3}, \quad \forall \theta, \widetilde{\theta} : [\varphi_{t,\theta}^{D} \leq \varphi_{t,\widetilde{\theta}}^{D}], \quad \forall t \quad \& \quad \Gamma_3 = \left[W, BS, (CA, dis), (CA, s) \right] \tag{38}$$

$$\sigma_{t,\theta}^{D,\Gamma_4} \leq \sigma_{t,\widetilde{\theta}}^{D,\Gamma_4}, \quad \forall \theta, \widetilde{\theta} : [\varphi_{t,\theta}^{D} \geq \varphi_{t,\widetilde{\theta}}^{D}], \quad \forall t \quad \& \quad \Gamma_4 = [BS, CA] \tag{39}$$

$$\chi_{t,\theta}^{D,\Gamma_3} = \chi_{t,\widetilde{\theta}}^{D,\Gamma_3}, \quad \forall \theta, \widetilde{\theta} : [\varphi_{t,\theta}^{D} = \varphi_{t,\widetilde{\theta}}^{D}], \quad \forall t \quad \& \quad \Gamma_3 = \left[W, BS, (CA, dis), (CA, s) \right] \tag{40}$$

$$\sigma_{t,\theta}^{D,\Gamma_4} = \sigma_{t,\widetilde{\theta}}^{D,\Gamma_4}, \quad \forall \theta, \widetilde{\theta} : [\varphi_{t,\theta}^{D} = \varphi_{t,\widetilde{\theta}}^{D}], \quad \forall t \quad \& \quad \Gamma_4 = [BS, CA] \tag{41}$$

$$\chi_{t,\theta}^{I,\Gamma_5} = \chi_{t,\widetilde{\theta}}^{I,\Gamma_5}, \quad \forall \theta, \widetilde{\theta} : [\varphi_{t,\theta}^{D} = \varphi_{t,\widetilde{\theta}}^{D}], \quad \forall t \quad \& \quad \Gamma_5 = \left[W, BS, (CA, dis), (CA, s) \right] \tag{42}$$

$$\sigma_{t,\theta}^{I,\Gamma_6} = \sigma_{t,\widetilde{\theta}}^{I,\Gamma_6}, \quad \forall \theta, \widetilde{\theta} : [\varphi_{t,\theta}^{D} = \varphi_{t,\widetilde{\theta}}^{D}], \quad \forall t \quad \& \quad \Gamma_6 = \left[W, BS, CA \right] \tag{43}$$

2.3. Problem formulation in the presence of degradation cost

Multiple charging and discharging cycles of the BES system are deemed as the most critical factors of reducing the BES lifespan, and as a result, the BES replacement cost should be taken into account. This is done by including the BES system degradation cost in its offering and bidding pattern. BES degradation is contingent on a variety of factors, whereas the cycle depth is identified as the most significant one [36]. In this paper, to incorporate the BES degradation cost into the preceding modeling, the model in [36] has been adopted. Accordingly, the degradation cost is modeled as a nonlinear function of the depth of discharge and a piecewise linearization method is employed to overcome its nonlinearity. The latest depth of discharge at each specific time can be tracked by devoting discharge and charge power components along with energy level component to any particular depth of discharge block concerning its present and former discharge and charge powers. Comprehensive details of this model with the benefits of its application have been thoroughly discussed in [36]. Eventually, the objective function (1) by considering the BES degradation cost is updated as:

$$\text{Max} \quad \text{PF}_2 = \text{PF}_1 - \sum_{\Theta=1}^{N_\theta} \sum_{b=1}^{N_B} \sum_{t=1}^{N_T} \pi_\theta \times \left[MC_b \times \varrho_{b,t,\theta}^{Sch,BS,dis} \right] \tag{44}$$

Subject to:

$$\chi_{t,\theta}^{D,BS} = \sum_{b=1}^{N_B} \varrho_{b,t,\theta}^{D,BS,dis} \tag{45}$$

$$\sigma_{t,\theta}^{D,BS} = \sum_{b=1}^{N_B} \varrho_{b,t,\theta}^{D,BS,ch} \tag{46}$$

$$\chi_{t,\theta}^{I,BS} = \sum_{b=1}^{N_B} \varrho_{b,t,\theta}^{I,BS,dis} \tag{47}$$

$$\sigma_{t,\theta}^{I,BS} = \sum_{b=1}^{N_B} \varrho_{b,t,\theta}^{I,BS,ch} \tag{48}$$

$$\varrho_{b,t,\theta}^{Sch,BS,dis} = \varrho_{b,t,\theta}^{D,BS,dis} + \varrho_{b,t,\theta}^{I,BS,dis} \tag{49}$$

$$\varrho_{b,t,\theta}^{Sch,BS,ch} = \varrho_{b,t,\theta}^{D,BS,ch} + \varrho_{b,t,\theta}^{I,BS,ch} \tag{50}$$

$$\chi_{t,\theta}^{Sch,BS,dis} = \sum_{b=1}^{N_B} \varrho_{b,t,\theta}^{Sch,BS,dis} \tag{51}$$

$$\sigma_{t,\theta}^{Sch,BS,ch} = \sum_{b=1}^{N_B} \varrho_{b,t,\theta}^{Sch,BS,ch} \tag{52}$$

$$\varrho_{b,t,\theta}^{D,BS,dis}, \varrho_{b,t,\theta}^{I,BS,dis}, \varrho_{b,t,\theta}^{D,BS,ch}, \varrho_{b,t,\theta}^{I,BS,ch} \geq 0 \tag{53}$$

$$ELL_{b,t,\theta}^{BS} = ELL_{b,t-1,\theta}^{BS} - \left(\frac{1}{\Upsilon^{BS,dis}} \right) \left(\varrho_{b,t,\theta}^{Sch,BS,dis} \right) + \Upsilon^{BS,ch} \left(\varrho_{b,t,\theta}^{Sch,BS,ch} \right), \quad \forall t, \forall \theta \tag{54}$$

$$0 \leq ELL_{b,t,\theta}^{BS} \leq ELL_{b}^{BS,Max} \tag{55}$$

$$EL_{t,\theta}^{BS} = \sum_{b=1}^{N_B} ELL_{b,t,\theta}^{BS} \tag{56}$$

$$- \text{PF}_{1,\theta} + \left(\sum_{b=1}^{N_B} \sum_{t=1}^{N_T} MC_b \times \varrho_{b,t,\theta}^{Sch,BS,dis} \right) + \gamma - \eta_\theta \leq 0, \quad \forall \theta \tag{57}$$

Constraints (2), (4)–(9), (11)–(43) (58)

where PF_2 is the objective function of the HPGS including the BES degradation cost. Eqs. (45) and (46) compute the selling (offering) and buying (bidding) quantities of the BES system in the DA market according to their discharging and charging powers in each block of the depth of discharge. Similar to (45) and (46), Eqs. (47) and (48) are adopted for intraday offering and bidding variables. The total offering and bidding values in each block of the depth of discharge are calculated via (49) and (50), whereas the total scheduled offering and bidding values of the BES system are computed through (51) and (52). The BES energy level in each block is obtained by (54), while constraint (55) restricts the lower and upper boundaries of this variable. The final energy level of the BES system is stated in (56), and restriction (57) is related to CVaR modeling. Some other constraints of the proposed methodology are unchanged, as stated in (58).

3. Simulation results

The performance of the suggested offering and bidding strategy is analyzed for an HPGS comprising a 50-MW wind farm, a BES facility of 50 MW (charging and discharging capacity), and a CAES unit of charging and discharging capacities equal to 100 MW and 150 MW, respectively. The technical information on CAES and BES facilities are reported in Table 1. The BES replacement cost is set to 300,000 €/MWh [36], while other relevant data for modeling degradation cost of the BES system are adopted from [36]. Six months of historical data (January 1st, 2018 to June 30th, 2018) of the electricity market in the Iberian Peninsula [37] and the wind speeds [38] for the same period are used for scenario generation. Following the procedures described in 2.1, 5000 scenarios are generated for each uncertain parameter and, using the scenario reduction technique, the number of scenarios for the DA, intraday, balancing markets, and wind power are reduced to 10, 6, 6, and 10 representative scenarios, respectively. Accordingly, the overall number of scenarios is 3600.

Three distinct DRRs have been considered for participation in the IDREX market. The maximum participation level for each DRR is assumed to be 4 MW. The parameters appertaining to price–quantity offers of DRRs in the IDREX market are based on three characteristic periods, namely, peak, off-peak, and valley, as given in Table 2. Note that the uncertainty of IDREX market prices is neglected (mean prices are considered here). Furthermore, the HPGS is capable of procuring energy through bilateral contracts from DRRs where $\varphi_{1,t}^{B}$, $\varphi_{1,t}^{B}$, and $\varphi_{3,t}^{B}$ are equal to 45, 50, and 55 €/MWh. Finally, other essential parameters in the proposed problem, such as α, λ, and NPG are respectively set to 0.95, 0.3, 4.6 €/MBtu. The derived problem is solved by GAMS under CPLEX solver.

In this paper, three case studies corresponding to three different offering and bidding schemes have been considered:

Table 1
Specification of CAES and BES facilities.

Parameter	Value	Unit	Parameter	Value	Unit
$Cap^{CA,exp}$	150	MW	Htr^{s}	10.83	MBtu/MWh
$Cap^{CA,c}$	100	MW	ER	0.95	Scalar
$EL^{CA,Max}$	20 × 150	MWh	OM^{Exp}	3	€/MWh
Htr^{dis}	4.07	MBtu/MWh	OM^{Com}	3	€/MWh
$\Upsilon^{BS,ch}$	80	%	$Cap^{BS,dis(ch)}$	50	MW
$\Upsilon^{BS,dis}$	95	%	$EL^{BS,Max}$	5 × 50	MWh

Table 2
Characteristic of DRRs' offer in the IDREX market.

Period	f	1	2	3
	$v^{Max}_{d,f,t}$	0.25 × Cap^{DR}_{d}	0.75 × Cap^{DR}_{d}	1 × Cap^{DR}_{d}
	Percentage of mean intraday market price			
Valley (1–9 a.m.)	$\varphi^{IX}_{1,f,t}$	45%	60%	75%
	$\varphi^{IX}_{2,f,t}$	50%	65%	80%
	$\varphi^{IX}_{3,f,t}$	55%	70%	85%
Off-peak (10 a.m.–19 p.m.)	$\varphi^{IX}_{1,f,t}$	55%	85%	115%
	$\varphi^{IX}_{2,f,t}$	65%	95%	125%
	$\varphi^{IX}_{3,f,t}$	75%	105%	135%
Peak (20–24 p.m.)	$\varphi^{IX}_{1,f,t}$	60%	90%	120%
	$\varphi^{IX}_{2,f,t}$	70%	100%	130%
	$\varphi^{IX}_{3,f,t}$	80%	110%	140%

- **Case 1**: disjoint operation of all available energy resources.
- **Case 2**: coordinated operation of wind, BES and CAES facilities.
- **Case 3**: coordinated operation of wind, BES and CAES facilities in the attendance of DRRs.

In order to thoroughly investigate different features of the suggested methodology, the numerical results are presented in two parts. In the first part, the profitability of the aforementioned offering and bidding schemes and the HPGS behavior in electricity markets are fully examined. In the second part, the impact of incorporating the BES degradation cost on the BES decisions in DA and intraday markets, as well as economic losses, are studied.

3.1. Results: Part I

In the following, the effects of different bidding schemes are examined. It is necessary to remark that the BES degradation cost has been overlooked in all results of the first part.

3.1.1. Impact of various offering and bidding cases on the expected profit and CVaR

Results of CVaR and expected profit for various values of β and different offering and bidding schemes have been reported in Tables 3 and 4. According to Tables 3 and 4, the HPGS's expected profit in the risk-neutral analysis of disjoint operation is €33,381.966, while the coordinated offering and bidding strategy in the second case leads to a 13.02% increase of expected profit. In the same way, in the second scheme, the system experiences an 8.39% gain in the CVaR, which illustrates that the system's risk is reduced by the coordinated operation. Using DRRs to cope with intermittent wind power generation via the IDREX market, improves both substantially, CVaR and expected profit. In this regard, for $\beta = 0$, the coordinated scheduling of existing units in the presence of the IDREX market results in a 22.11% and a 23% increase in expected profit and CVaR, respectively. Adopting a more conservative scheduling, i.e., increasing parameter β [39], reduces the value of expected profit and increases the value of CVaR. Accordingly, in the third operational case, by altering $\beta = 0$ to $\beta = 1$, this case produces only a 0.28% reduction in system's profit, while it increases the CVaR value by 20.75%. This demonstrates the efficiency of the proposed offering and bidding mechanism. In other words, a slight loss in the expected profit can be used by the decision-maker to remarkably reduce the associated risk.

Table 4
Expected profit and CVaR gain in $\beta = 0$.

Case studies	Gain (%)	
	Expected profit	CVaR
Case 2	13.02	8.39
Case 3	22.11	23.00

Table 5
Impact of coordinated and disjoint operation of the CAES on the expected profit and CVaR of the HPGS.

Case study	Expected profit (€)		CVaR (€)	
	$\beta = 0$	$\beta = 2$	$\beta = 0$	$\beta = 2$
Coordinated [Wind-BES] + disjoint CAES	35,132.189	34,720.782	22,802.951	26,463.441
HPGS	37,728.841	37,394.281	23,347.454	29,173.620

To further analyze the benefits of the CAES on the operation of the HPGS (Case 2), Table 5 reports the impact of integrating CAES on the expected profit and CVaR of the HPGS. This analysis is performed for two different values of β ($\beta = 0$ and $\beta = 2$). As can be seen, the CAES plays a significant role in boosting the expected profit and CVaR of the HPGS, showing the benefits of entering the CAES into the proposed HPGS. According to this table, the presence of the CAES in the HPGS results in a 7.38% and a 2.38% in expected profit and CVaR of the risk-neutral analysis ($\beta = 0$), respectively. Similarly, these values for $\beta = 2$ are increased to 7.69% (expected profit) and 10.24% (CVaR), implying the more substantial role of the CAES in the conservative scheduling. Overall, the CAES increases profitability and reduces the associated risk.

3.1.2. Impact of various offering and bidding cases on the DA decisions

In order to illustrate how various decision-making schemes affect DA variables, the expected offering and bidding quantities in the DA market for the wind farm, CAES, and BES facilities pertaining to risk-neutral analysis are depicted in Fig. 3. Applying a coordinated operation of all resources (second and third cases), shows that the DA decisions of the wind farm are mostly altered. In this regard, the wind farm offers in the second and the third cases during the whole

Table 3
Expected profit and CVaR in different case studies.

Case study		Expected profit (€)				CVaR (€)			
		$\beta = 0$	$\beta = 0.5$	$\beta = 1$	$\beta = 2$	$\beta = 0$	$\beta = 0.5$	$\beta = 1$	$\beta = 2$
Case 1	Wind farm	26,285.126	26,181.438	26,098.283	25,991.201	18,490.960	20,470.339	20,592.013	20,671.606
	CAES	5162.011	5157.579	5104.937	5068.048	2622.630	2816.622	2870.622	2906.622
	BES	1934.829	1928.811	1927.122	1926.981	424.952	745.640	748.352	748.476
	Sum	33,381.966	33,267.828	33,130.342	32,986.23	21,538.542	24,032.601	24,210.987	24,326.704
Case 2	HPGS	37,728.841	37,621.710	37,551.382	37,394.281	23,347.454	29,022.289	29,121.190	29,173.620
Case 3	HPGS+DRRs	40,763.112	40,647.770	40,567.847	40,531.028	26,492.865	31,992.368	32,108.421	32,127.062

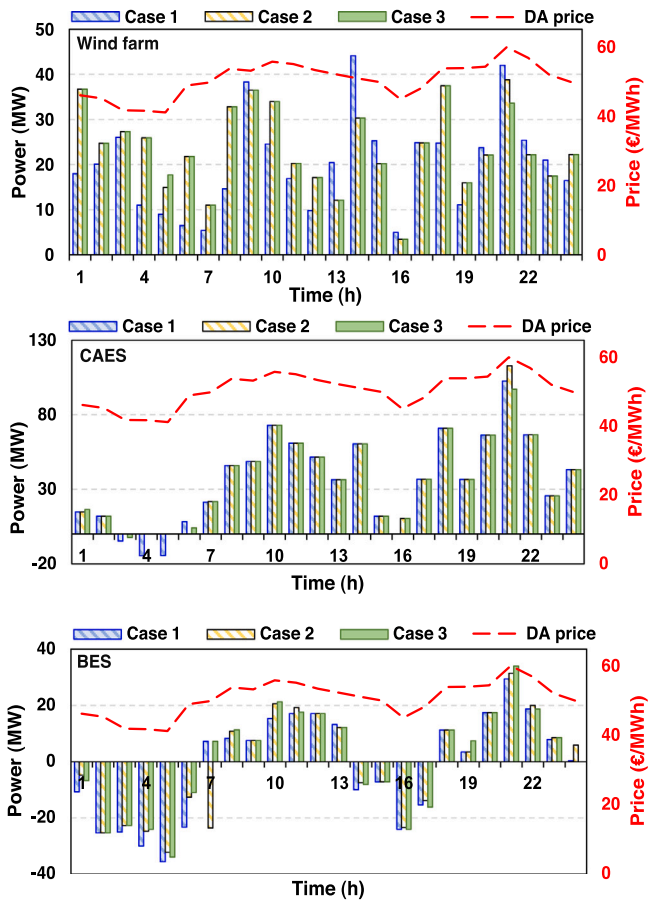

Fig. 3. Expected offering and bidding quantities of the HPGS in the DA market.

scheduling horizon are the same, except for hours 5 and 21. This fact illustrates how considering DRRs in the IDREX market can alter the system's decisions in the DA market. Another important point of attention is that the participation of two energy storage systems, i.e., BES and CAES, in the DA market is quite different from each other. The BES system relies on purchasing energy at hours with low energy prices and selling energy during high price hours, while the CAES facility mainly operates in the simple-cycle mode since its charging power is extremely low during the 24-hour horizon. The highest charging and discharging powers of the BES facility happens at hours 5 and 21 with the lowest and highest energy prices, respectively.

The DA offering and bidding curves are the key outputs of the proposed method. These curves for two specific hours and two different risk levels are shown in Fig. 4. As can be seen, different scheduling cases and risk levels lead to diverse offering and bidding curves. In the risk-neutral analysis ($\beta = 0$), the bidding quantities of the second and the third scheduling cases are lower than or equal the corresponding quantities in the first case, while the system's offering values in the second and the third cases for price realizations higher than €57.2/MWh are higher than in case 1. Also in the risk-aversion case ($\beta = 2$), the generation offers of the HPGS at hour 22 increase for two price realizations, i.e., €54.88/MWh and €57.2/MWh, while its offering curve in the first case does not change in comparison with the risk-neutral analysis.

3.1.3. Impact of various offering and bidding cases on the intraday decisions

The total traded energy in the intraday market for all scheduling cases and various values of β are presented in Fig. 5. The total traded energy in the first case has a positive value for all risk aversion levels, indicating that the total amount of power sold is higher than the amount of power purchased in this market. In the second case, the total amount of energy sold in this market is decreased, and, subsequently, by increasing the value of β, the system concentrates on purchasing electricity rather than selling it in the intraday market. Finally, in the last case, the total traded energy for both risk-neutral and risk aversion cases is negative due to the availability of the IDREX market. Fig. 6 shows the optimal procured pool-based and bilateral-based energy from DRRs in the third case. It can be seen that the power provided during the valley period is at its highest limit due to the low price offers of DRRs in this period. Despite changing parameter β, the bilateral-based energy does not change, while the pool-based energy merely experiences slight variations during off-peak and peak periods.

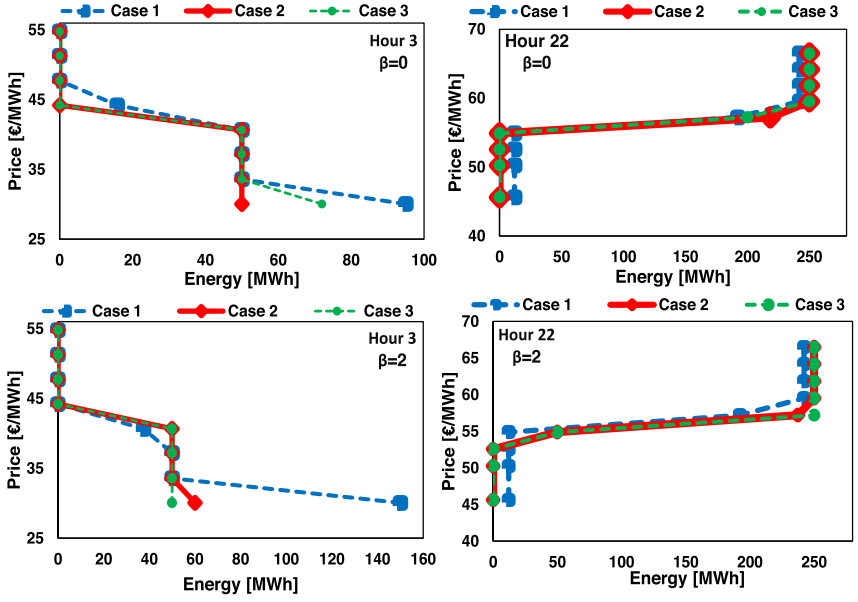

Fig. 4. Offering and bidding curves of the HPGS in the DA market for hours 3 and 22.

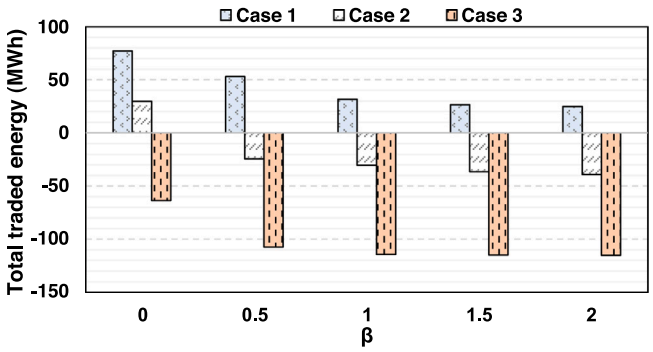

Fig. 5. Total traded energy in the intraday market for different values of β.

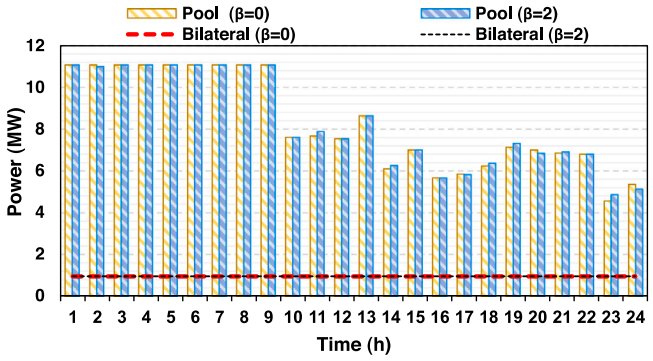

Fig. 6. Optimal traded energy between the HPGS and DRRs in the third case.

3.1.4. Impact of various offering and bidding cases on the imbalances

The effects of the different scheduling cases and diverse risk-aversion levels on the last-stage decisions of the developed offering and bidding structure, namely, imbalance cost and total energy deviations are shown in Fig. 7. By comparing the imbalance cost for different values of β, we can conclude that the more conservative the policy is, the more eager the system becomes to reduce the imbalance cost, and, thus, increase its profitability in the balancing market. From this figure, it is observed that the imbalance cost of the HPGS in the second offering and bidding case increases in comparison with the first one. This is due to the fact that the coordinated scheduling of existing units lets the system take action more freely in the target markets which, accordingly, despite the rising imbalance cost, increases the system's expected profit. However, as can be seen from Fig. 7, the third operational case can be used to considerably reduce the imbalance cost of the second case by providing energy from DRRs in the IDREX market. It should be noted that the results of total deviations in the balancing market are inversely related to the imbalance cost in the aforementioned market. It is also worth mentioning that positive values of energy deviations reflect the excess of generated energy in the balancing market which should be sold in this market, while negative values represent the shortage of delivered energy in the balancing market with respect to the scheduled energy that needs to be purchased from this market. For instance, as the total energy deviations increase (increasing β), the imbalance cost reduces. Similarly, the highest negative energy deviation concerns the second operational case with the highest imbalance cost.

3.2. Results: Part II

In this part, the influence of adding the BES degradation cost on the proposed methodology is investigated. As previously stated in 2.3, to keep the model linear, the degradation cost curve is linearized by means of 20 blocks. Table 6 reports the results of considering or ignoring the BES degradation cost for two specific case studies, namely,

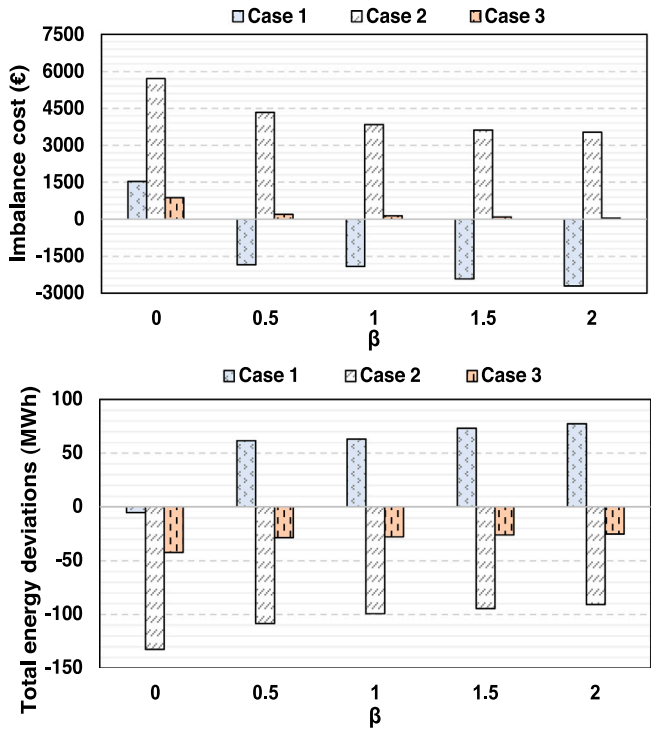

Fig. 7. Expected imbalance cost and total energy deviations in the balancing market for different values of β.

Table 6
Economic impacts of the BES degradation cost on two specific case studies.

Case studies	Expected profit (€)	Expected degradation cost (€)	CVaR (€)
Case 1: BES without degradation cost	1934.829	0	424.952
Case 1: BES with degradation cost	1869.419	62.531	382.926
Case 3 without degradation cost	40,763.112	0	26,492.865
Case 3 with degradation cost	40,693.201	67.206	26,436.749

uncoordinated (Case 1) and coordinated (Case 3) operations. According to these results, considering the BES degradation imposes economic losses of €62.531 and €67.206 on uncoordinated and coordinated operations, respectively. Not surprisingly, the CVaR also decreases by taking into account the BES degradation. Moreover, the greater degradation cost of Case 3 reveals that this strategy has deeper depth of discharges compared to Case 1. The expected profit values and corresponding CVaR values for Case 3 with degradation cost under various values of β are depicted in Fig. 8. As seen, by increasing the value of β, CVaR values are increased, while expected profit values are decreased.

Figs. 9 and 10 illustrate the BES offering and bidding quantities in DA and intraday markets, respectively. As reported by these figures, all in all, Case 3 experiences greater depth of discharges in comparison with Case 1. Furthermore, by comparing the offering and bidding quantities of the BES system with and without degradation in Case 1, it is observed that offering and bidding values in both DA and intraday markets decrease if we take into account the degradation cost. Following this, smaller bidding quantities in both DA and intraday markets are noted when counting the degradation cost in Case 3. Also, a comparison between the offering values in the DA and intraday markets with and without taking into account BES degradation lets us conclude

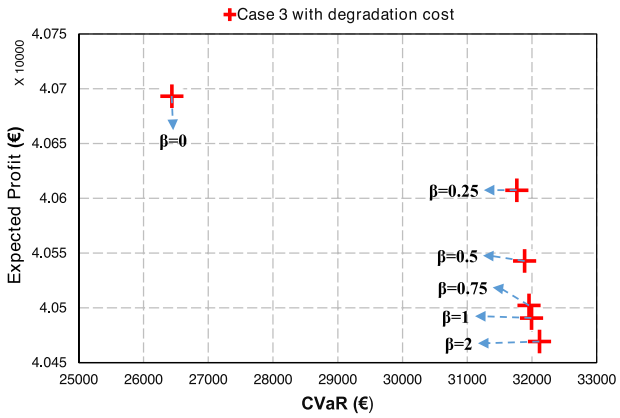

Fig. 8. Expected profit and CVaR for various values of β in Case 3 with degradation cost.

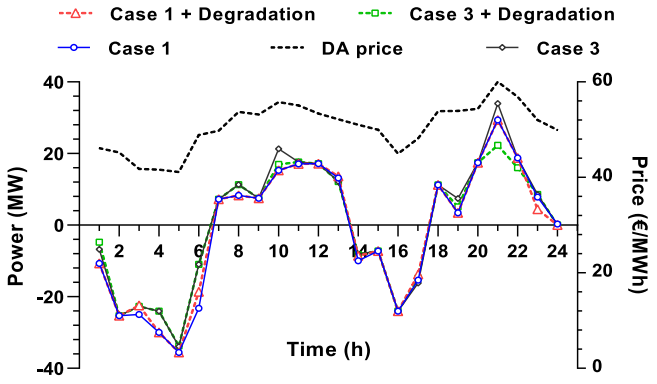

Fig. 9. Expected offering and bidding quantities of the BES in the DA market by considering and ignoring the BES degradation.

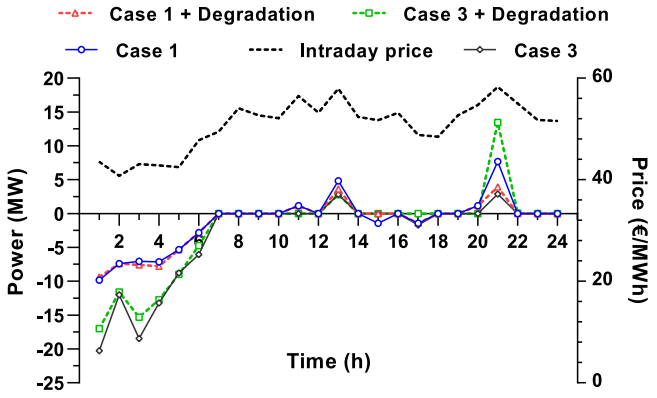

Fig. 10. Expected offering and bidding quantities of the BES in the intraday market by considering and ignoring the BES degradation.

that degradation considerations lead to higher intraday and lower DA offering values. Lastly, the model statistics in Case 3 with degradation cost are given in Table 7. Note that all simulations have been performed in an ASUS laptop with 8 GB of RAM and a Core i5 CPU. As seen, the computation time is acceptable, and the model has been scaled well.

4. Conclusions and future work

In this paper, a comprehensive joint offering and bidding mechanism was presented for an HPGS comprising of BES and CAES facilities together with wind units and energy transactions with DRRs. The proposed model was formulated as a three-stage stochastic MILP problem and a practical risk management index, i.e., CVaR, was included in the suggested structure. Diverse case studies based on various offering and bidding schemes were designed, and different aspects of solutions were studied. The main observations are:

- The impact of coordinated operation of wind, BES and CAES resources on profit gain is more significant than the CVaR gain, while using energy transactions between the HPGS and DRRs in the proposed scheduling framework leads to a similar increase of expected profit and CVaR, i.e., 22.11% and 23%, respectively.
- The coordinated participation of all resources in the electricity markets has the most considerable influence on DA decisions of the wind farm. In this regard, various risk-aversion levels and different operational schemes give rise to variations in the offering and bidding curves.
- The share of intraday energy market sales in the disjoint strategy is higher than in the coordinated one. Furthermore, adopting a more conservative approach increases the system's tendency to purchase energy from this market.
- The coordinated offering and bidding model allows a more flexible involvement of the HPGS in the DA and intraday markets by increasing downward imbalances in the balancing market aiming for a higher profit. In this regard, the IDREX market proves to be a useful tool to dramatically lower the imbalance cost imposed on the system.
- The BES system experiences a deeper depth of discharge in the coordinated operation compared to the uncoordinated one, which results in a greater degradation cost.

For future work, we plan to incorporate power-to-gas facilities into the proposed HPGS and establish an appropriate offering and bidding mechanism to enlarge the system's flexibility and profitability. Further, providing balancing reserves in addition to balancing energy could be another perspective for future research directions.

Table 7
Model statistics in Case 3 with degradation cost.

Number of continuous variables	56,385
Number of binary variables	120
Number of equations variables	73,034
Computation time	5.9 s

CRediT authorship contribution statement

Hooman Khaloie: Conceptualization, Methodology, Software, Data curation, Writing – original draft. **Amjad Anvari-Moghaddam:** Formal analysis, Methodology, Supervision, Writing – review & editing. **Javier Contreras:** Methodology, Supervision, Writing – review & editing. **Jean-François Toubeau:** Methodology, Supervision, Writing – review & editing. **Pierluigi Siano:** Methodology, Supervision, Writing - review & editing. **François Vallée:** Methodology, Supervision, Writing – review & editing.

Declaration of competing interest

The authors declare that they have no known competing financial interests or personal relationships that could have appeared to influence the work reported in this paper.

References

[1] Samal RK, Tripathy M. Cost savings and emission reduction capability of wind-integrated power systems. Int J Electr Power Energy Syst 2019;104:549–61.
[2] Agrali C, Gultekin H, Tekin S, Oner N. Measuring the value of energy storage systems in a power network. Int J Electr Power Energy Syst 2020;120:106022.

[3] Child M, Bogdanov D, Breyer C. The role of storage technologies for the transition to a 100% renewable energy system in Europe. Energy Procedia 2018;44–60. http://dx.doi.org/10.1016/j.egypro.2018.11.067.
[4] Bottieau J, Hubert L, De Grève Z, Vallée F, Toubeau J-F. Very-short-term probabilistic forecasting for a risk-aware participation in the single price imbalance settlement. IEEE Trans Power Syst 2019;35:1218–30.
[5] Cao D, Hu W, Xu X, Dragičević T, Huang Q, Liu Z, et al. Bidding strategy for trading wind energy and purchasing reserve of wind power producer–A DRL based approach. Int J Electr Power Energy Syst 2020;117:105648.
[6] AlAshery MK, Xiao D, Qiao W. Second-order stochastic dominance constraints for risk management of a wind power producer's optimal bidding strategy. IEEE Trans Sustain Energy 2019. http://dx.doi.org/10.1109/tste.2019.2927119.
[7] Aghaei J, Barani M, Shafie-Khah M, Sanchez De La Nieta AA, Catalao JPS. Risk-constrained offering strategy for aggregated hybrid power plant including wind power producer and demand response provider. IEEE Trans Sustain Energy 2016;7:513–25. http://dx.doi.org/10.1109/TSTE.2015.2500539.
[8] Khaloie H, Mollahassani-pour M, Anvari-Moghaddam A. Optimal behavior of a hybrid power producer in day-ahead and intraday markets: A bi-objective cvar-based approach. IEEE Trans Sustain Energy 2020;1. http://dx.doi.org/10.1109/TSTE.2020.3026066.
[9] Fan W, Huang L, Cong B, Degejirifu, Tan Z, Xing T. Research on an optimization model for wind power and thermal power participating in two-level power market transactions. Int J Electr Power Energy Syst 2022;134:107423. http://dx.doi.org/10.1016/J.IJEPES.2021.107423.
[10] Pei W, Du Y, Deng W, Sheng K, Xiao H, Qu H. Optimal bidding strategy and intramarket mechanism of microgrid aggregator in real-time balancing market. IEEE Trans Ind Inform 2016;12:587–96. http://dx.doi.org/10.1109/TII.2016.2522641.
[11] Mirzaei MA, Hemmati M, Zare K, Abapour M, Mohammadi-Ivatloo B, Marzband M, et al. A novel hybrid two-stage framework for flexible bidding strategy of reconfigurable micro-grid in day-ahead and real-time markets. Int J Electr Power Energy Syst 2020;123:106293.
[12] Samadi Gazijahani F, Salehi J. IGDT based complementarity approach for dealing with strategic decision making of price maker VPP considering demand flexibility. IEEE Trans Ind Inform 2019. http://dx.doi.org/10.1109/tii.2019.2932107.
[13] Vahedipour-Dahraie M, Rashidizadeh-Kermani H, Anvari-Moghaddam A, Siano P. Risk-averse probabilistic framework for scheduling of virtual power plants considering demand response and uncertainties. Int J Electr Power Energy Syst 2020;121:106126.
[14] Hasankhani A, Hakimi SM. Stochastic energy management of smart microgrid with intermittent renewable energy resources in electricity market. Energy 2021;219:119668.
[15] Arteaga J, Zareipour H. A price-maker/price-taker model for the operation of battery storage systems in electricity markets. IEEE Trans Smart Grid 2019;10:6912–20.
[16] Attarha A, Amjady N, Dehghan S. Affinely adjustable robust bidding strategy for a solar plant paired with a battery storage. IEEE Trans Smart Grid 2019;10:2629–40. http://dx.doi.org/10.1109/TSG.2018.2806403.
[17] Khaloie H, Abdollahi A, Shafie-khah M, Anvari-Moghaddam A, Nojavan S, Siano P, et al. Coordinated wind-thermal-energy storage offering strategy in energy and spinning reserve markets using a multi-stage model. Appl Energy 2019;114168. http://dx.doi.org/10.1016/J.APENERGY.2019.114168.
[18] Khatami R, Oikonomou K, Parvania M. Look-ahead optimal participation of compressed air energy storage in day-ahead and real-time markets. IEEE Trans Sustain Energy 2019.
[19] Attarha A, Amjady N, Dehghan S, Vatani B. Adaptive robust self-scheduling for a wind producer with compressed air energy storage. IEEE Trans Sustain Energy 2018;3029. http://dx.doi.org/10.1109/TSTE.2018.2806444.
[20] Jirsaraie SG, Ghadi MJ, Vahed AA, Aghaei J, Li L, Zhang J. Risk-constrained bidding strategy for a joint operation of wind power and compressed air energy storage aggregators. IEEE Trans Sustain Energy 2019.
[21] Abbasi MH, Taki M, Rajabi A, Li L, Zhang J. Coordinated operation of electric vehicle charging and wind power generation as a virtual power plant: A multi-stage risk constrained approach. Appl Energy 2019. http://dx.doi.org/10.1016/j.apenergy.2019.01.238.
[22] Khaloie H, Abdollahi A, Rashidinejad M. Risk-constrained self-scheduling and forward contracting under probabilistic-possibilistic uncertainties. In: Electr. eng. (ICEE), iran. conf.. IEEE; 2018, p. 1138–43. http://dx.doi.org/10.1109/ICEE.2018.8472668.
[23] Khaloie H, Abdollahi A, Rashidinejad M, Siano P. Risk-based probabilistic-possibilistic self-scheduling considering high-impact low-probability events uncertainty. Int J Electr Power Energy Syst 2019;110:598–612. http://dx.doi.org/10.1016/j.ijepes.2019.03.021.
[24] MollahassaniPour M, Taheri I, Marzooni MH. Assessment of transmission outage contingencies' effects on bidding strategies of electricity suppliers. Int J Electr Power Energy Syst 2020;120:106053.
[25] Khaloie H, Anvari-Moghaddam A. Robust optimization approach for generation scheduling of a hybrid thermal-energy storage system. In: 2020 IEEE 29th int symp ind electron. 2020, p. 971–6. http://dx.doi.org/10.1109/ISIE45063.2020.9152266.
[26] Sharifi R, Anvari-Moghaddam A, Fathi SH, Vahidinasab V. A bi-level model for strategic bidding of a price-maker retailer with flexible demands in day-ahead electricity market. Int J Electr Power Energy Syst 2020;121:106065.
[27] Zhang R, Jiang T, Li F, Li G, Chen H, Li X. Bi-level strategic bidding model for P2G facilities considering a carbon emission trading scheme-embedded LMP and wind power uncertainty. Int J Electr Power Energy Syst 2021;128:106740.
[28] Golmohamadi H, Keypour R, Bak-Jensen B, Pillai JR, Khooban MH. Robust self-scheduling of operational processes for industrial demand response aggregators. IEEE Trans Ind Electron 2019;67:1387–95.
[29] Liu W, Wen F, Qi D. Intraday residential demand response scheme based on peer-to-peer energy trading. IEEE Trans Ind Inform 2019.
[30] Khaloie H, Vallée F, Lai CS, Toubeau J-F, Hatziargyriou ND. Day-ahead and intraday dispatch of an integrated biomass-concentrated solar system: A multi-objective risk-controlling approach. IEEE Trans Power Syst 2021. http://dx.doi.org/10.1109/TPWRS.2021.3096815.
[31] Khaloie H, Abdollahi A, Nojavan S, Shafie-Khah M, Anvari-Moghaddam A, Siano P, et al. Offering strategy of thermal-photovoltaic-storage based generation company in day-ahead market. In: Electr. mark.. Springer; 2020, p. 113–33.
[32] Conejo AJ, Carrión M, Morales JM. Decision making under uncertainty in electricity markets. Vol. 1. Boston, MA: Springer US; 2010, http://dx.doi.org/10.1007/978-1-4419-7421-1.
[33] Khaloie H, Anvari-Moghaddam A, Contreras J, Siano P. Risk-involved optimal operating strategy of a hybrid power generation company: A mixed interval-cvar model. Energy 2021;232:120975. http://dx.doi.org/10.1016/j.energy.2021.120975.
[34] Hakimi SM, Hasankhani A, Shafie-khah M, Catalão JPS. Stochastic planning of a multi-microgrid considering integration of renewable energy resources and real-time electricity market. Appl Energy 2021. (accepted).
[35] Khaloie H, Abdollahi A, Shafie-Khah M, Siano P, Nojavan S, Anvari-Moghaddam A, et al. Co-optimized bidding strategy of an integrated wind-thermal-photovoltaic system in deregulated electricity market under uncertainties. J Clean Prod 2020;242:118434. http://dx.doi.org/10.1016/j.jclepro.2019.118434.
[36] Xu B, Zhao J, Zheng T, Litvinov E, Kirschen DS. Factoring the cycle aging cost of batteries participating in electricity markets. IEEE Trans Power Syst 2018;33:2248–59. http://dx.doi.org/10.1109/TPWRS.2017.2733339.
[37] Bienvenido | ESIOS electricidad · datos · transparencia. 2019, https://www.esios.ree.es/es (accessed March 14, 2019).
[38] Weather history+ - meteoblue. 2019, https://www.meteoblue.com/en/historyplus (accessed April 22, 2019).
[39] Khaloie H, Anvari-Moghaddam A, Hatziargyriou N, Contreras J. Risk-constrained self-scheduling of a hybrid power plant considering interval-based intraday demand response exchange market prices. J Clean Prod 2021;282:125344. http://dx.doi.org/10.1016/j.jclepro.2020.125344.